Available online at www.sciencedirect.com

SciVerse ScienceDirect

Ceramics International 39 (2013) 5705–5712

CERAMICS INTERNATIONAL

www.elsevier.com/locate/ceramint

Development of electrically conductive zirconia Part1: The optimal process parameters and mechanical properties

Shi-Yung Chiou[a,*], Cui-Feng Wang[b], Shih-Fu Ou[a,c,d], Keng-Liang Ou[c,d,e,**], Zhang-Ting Tsai[a]

[a]*Department of Mold and Die Engineering, National Kaohsiung University of Applied Science, 415 Chien Kung Road, Kaohsiung 807, Taiwan*
[b]*Department of Mechanical and Electrical Engineering, Fujian Polytechnic of Information Technology, Fuzhou 350003, China*
[c]*Research Center for Biomedical Devices and Prototyping Production, Taipei Medical University, Taipei 110, Taiwan*
[d]*Graduate Institute of Biomedical Materials and Tissue Engineering, College of Oral Medicine, Taipei Medical University, Taipei 110, Taiwan*
[e]*Research Center for Biomedical Implants and Microsurgery Devices, Taipei Medical University, Taipei 110, Taiwan*

Received 3 November 2012; received in revised form 28 December 2012; accepted 29 December 2012
Available online 9 January 2013

Abstract

The Taguchi method was applied to analyze the optimum process parameters of a 3 mol% yttria-tetragonal zirconia polycrystal (3Y-TZP) containing 30 wt% titanium nitride (TiN) (3Y-TZP/TiN). Four process parameters—(1) sintering type, (2) crushing time of TiN powder, (3) the first-step sintering duration, and (4) the second-step sintering temperature were chosen as the controlling factors. Fracture toughness, flexural strength, hardness, relative density, and electric resistance were examined using an L_9 orthogonal array. The results indicated that the fracture toughness was mainly affected by the duration of the first sintering step. The highest fracture toughness (9.275 MPa $m^{1/2}$) was achieved at 97.3 vol% of the tetragonal phase in 3Y-TZP/TiN. In addition, 3Y-TZP/TiN possessing a high fracture toughness of 8.59 MPa $m^{1/2}$ and a flexural strength of 680.77 MPa was fabricated using the optimum process parameters, 8 h crushing time of TiN powder, and the two-step sintering process. The electric resistance for 3Y-TZP/TiN was $3.26 \times 10^{-3}\ \Omega$ cm.

Keywords: Electrically conductive zirconia; Taguchi method; Fracture toughness

1. Introduction

Yttria-stabilized zirconia polycrystal (Y-TZP), particularly Y-TZP containing 3 mol% Y_2O_3, commonly called 3Y-TZP, has been widely studied and applied for several years [1–3]. Recently, to meet the production demands for general circuits, integrated circuit substrates, micro-motors, and micro-stamping parts in optoelectronic applications, the mold life-span and machine precision had to be improved by enhancing the punch capability of anti-sticking techniques against tin, copper, nickel, and other metals during the stamping process. Y-TZP has superior anti-sticking characteristics during the stamping process over tungsten carbide/cobalt (WC/Co). Furthermore, zirconia-based ceramics possess a slightly higher melting temperature (T_m) of 2700 °C and a significantly lower thermal conductivity (α) of 2.9 W/(m K) than WC/Co [4,5] ($T_m = 2860$ °C and $\alpha = 90$ W/m K). Therefore, under identical working conditions, zirconia-based ceramics, with their lower thermal conductivity, have a higher erosion rate than WC/Co when electricity is applied. Zirconia-based ceramics thus have greater potential for applications in molds and super-hard dies if electric discharge machining (EDM) is used.

Recently, the EDM technology has been applied as an acceptable procedure in the manufacturing of conductive ceramics [6]. Generally, a material that is machined using EDM requires a resistivity of less than 100 Ω cm [7]. However, the resistivity of zirconia is approximately 10^9–$10^{10}\ \Omega$ cm; therefore, electrically conductive second phases had to be added into the zirconia matrix. Previous studies

*Corresponding author. Tel.: +886 7 23814526 5430; fax: +886 7 3835015.
**Co-Corresponding author.
E-mail address: sychiou@cc.kuas.edu.tw (S.-Y. Chiou).

0272-8842/$ - see front matter © 2013 Elsevier Ltd and Techna Group S.r.l. All rights reserved.
http://dx.doi.org/10.1016/j.ceramint.2012.12.088

indicated that WC, TiC, and TiCN were good conductive media for zirconia and these zirconia-based ceramic composites were satisfied for EDM [8–10]. In addition, the influences of characteristics of the second phases on the EDM performance were investigated [7]. However, the mechanical properties of the electrically conductive zirconia-based ceramic composites and the optimum process parameters were not mentioned in previous studies.

According to research studies on the foundation and applications for Y-TZP containing TiN (Y-TZP/TiN) [11–13], the fracture toughness for Y-TZP/TiN obtained using a normal powder metallurgy process was as low as < 8 MPa $m^{1/2}$ [14–16], without using modified processes such as hot pressing or hot isostatic pressing. Moreover, its application was limited. Therefore, improving the fracture toughness is crucial for the manufacture of ceramic composites.

This study used the Taguchi methods to design experimental parameters, the sintering method, particle size, sustained heating time, and sintering temperature, as well as to inspect mechanical properties such as the fracture toughness, hardness, flexural strength, and the electric resistivity of the tested specimens after sintering.

2. Experimental procedure

ZrO_2 powder partially stabilized by 3 mol% Y_2O_3 (3Y-TZP) was used in this study. The 3Y-TZP powder (0.65 μm) was mixed with 30 wt% TiN powder. TiN powder (2 μm) was crushed using a three-dimensional crushing machine, and the particle size of TiN powder was measured using a laser nanoparticle analyzer. The mixed powder was then pressed in a stainless steel mold (10 mm in diameter) under a hydraulic pressure of 200 MPa for 1 min. Pressing was followed by the consolidation of the green compacts by ambient pressure sintering performed in nitrogen gas using a vacuum furnace. To avoid the sintered compacts' distortion caused by excessive heat, the heating rate was set at 10 °C/min during sintering and 5 °C/min during cooling. The

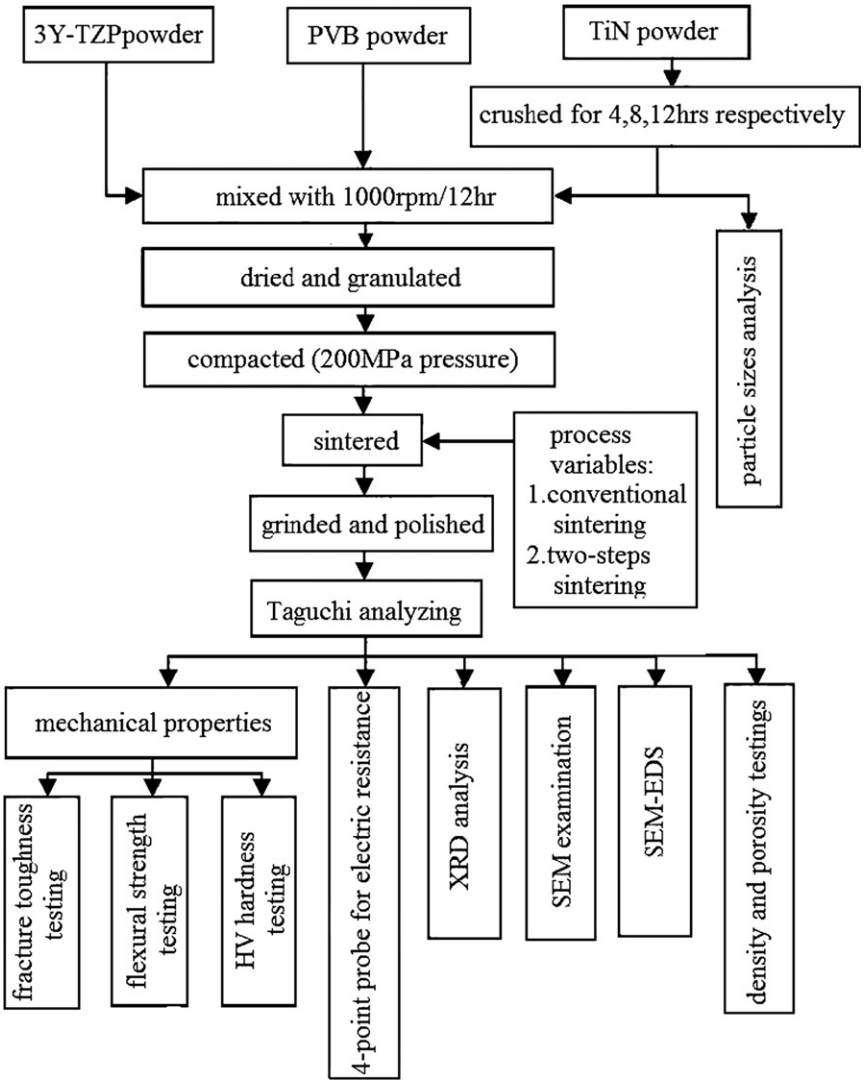

Fig. 1. Experimental flow chart.

Table 1
Experimental programming of Taguchi methods, L_9.

No.	Sample	A: Sintering type	B: TiN crushing time (hrs)	C: Duration time for the first step at 1450 °C(h)	D: Sintering temperature for the second step (°C)
Exp. 1	ZTN-1	Conventional sintering at 1450 °C (no duration time for the second step)	4	2	–
Exp. 2	ZTN-2	Conventional sintering at 1450 °C (no duration time for the second step)	8	1	–
Exp. 3	ZTN-3	Conventional sintering at 1450 °C (no duration time for the second step)	12	0	–
Exp. 4	ZTN-4	Two steps sintering (10 hours duration time for the second step)	4	1	1050
Exp. 5	ZTN-5	Two steps sintering (10 hours duration time for the second step)	8	0	1250
Exp. 6	ZTN-6	Two steps sintering (10 hours duration time for the second step)	12	2	1150
Exp. 7	ZTN-7	Two steps sintering (20 hours duration time for the second step)	4	0	1150
Exp. 8	ZTN-8	Two steps sintering (20 hours duration time for the second step)	8	2	1050
Exp. 9	ZTN-9	Two steps sintering (20 hours duration time for the second step)	12	1	1250

experimental procedures are outlined in Fig. 1. The conventional and first-step sintering temperature was 1450 °C. Three kinds of second-step sintering temperature were selected in this study, that is 1050 °C, 1150 °C, and 1250 °C.

The relative density of the sintered compacts was measured by the Archimedes' method. The Vickers hardness of the compacts was measured using a hardness tester (MVK-H1, Mitutoyo, Japan). Before hardness tests, the samples surface were polished by diamond lapping films with particle size from 30 μm to 3 μm. Indentations were performed on polished surfaces for an interval of 15 s. Higher loads were avoided because they resulted in extensive cracking. The fracture toughness (K_{IC}) was determined by measuring the length of the crack using the indentation fracture method [17]. The elastic modulus of 3Y-TZP and TiC used for calculating fracture toughness was 220 GPa and 430 GPa, respectively. The flexural strength was determined by a 3-point bending test using a universal testing machine (UH-1, Shimadzu, Japan). The specimen length was 40 mm, the thickness was 3 mm, and the cross-head speed was 0.5 mm/min according to the testing standard JIS R1601. In this study, six samples were used for each sintering process to obtain the average values. The electrical resistivity was determined by 4-point probe measurement (RT70) using an input voltage of 1 V and a current of 100 mA.

The surface morphologies of the sintering ceramic composites were observed by a scanning electron microscope (SEM) after thermal etching at 1380 °C for 20 min. The phases of the sintered compacts were characterized by X-ray diffractometry (XRD) (Model 2200, Rigaku, Japan). Monochromatic Cu K_α radiation was used at operating settings of 40 kV and 30 mA. The XRD data were collected over the 2θ range of 25°–85° at a step size of 0.04°/step and a counting time of 5 s. The volume percent of monoclinic ZrO2 (m-ZrO_2) was calculated by the following equations:

$$X_m = \frac{I_m(111)}{I_m(111)+I_m(-111)+I_t\,(111)} \tag{1}$$

$$V_m = \frac{1.31X_m}{1+0.31X_m} \tag{2}$$

I: Intensity of diffraction peak in the XRD pattern; V_m: the volume percent of m-ZrO_2.

This study used the Taguchi design to examine the effects of the manufacturing parameters on the zirconia characteristics such as hardness, flexural strength, fracture toughness, and resistivity. Four process parameters were used: (1) sintering type (referred to as Factor A below); (2) TiN powder crushing time or particle size (Factor B); (3) duration of the first step during sintering (Factor C); and (4) temperature of the second step during sintering (Factor D). Each parameter had three levels. For Factor A, the three levels were, in order: A1, single-stage sintering at 1450 °C; A2, two-step sintering comprising sintering at 1450 °C in the first stage and then kept at a certain temperature for 10 h in the second stage; and A3, two-step sintering comprising sintering at 1450 °C in the first stage and then kept at a certain temperature for 20 h in the second stage. For Factor B, the three levels were the crushing time of TiN power in the order of 4 h, 8 h, and 12 h. For Factor C, the duration for the sintering in the first step were, in order: 2 h, 1 h, and 0 h. For Factor D, the three levels were 1050 °C, 1250 °C, and 1150 °C. In sum, an L_9 array was adopted and is listed in Table 1. For the sintering specimens obtained by the nine experiments,

Table 2
Particle sizes (μm) and distribution of TiN powder after crushing.

Crushing time	Particle size (μm)/percentage (%)	Particle size (μm)/percentage (%)	Particle size (μm)/percentage (%)	Particle size (μm)/percentage
4 h	0.303/40	0.991/24	3.535/36	–
8 h	0.293/45	1.002/21	3.043/12	9.837/22%
12 h	0.264/53	0.954/16	5.588/31	–

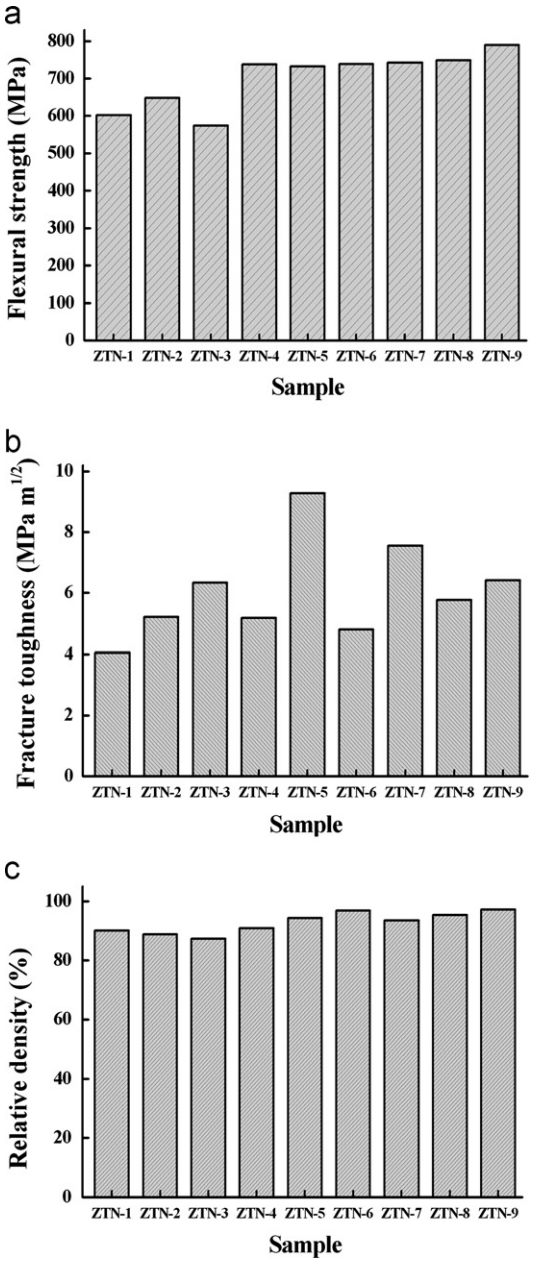

Fig. 2. The average (a) flexural strength, (b) fracture toughness and (c) relative density of sintered ceramic composites.

this study examined their characteristics such as flexural strength and fracture toughness, which were used to calculate the signal-to-noise ratio (S/N) for each experiment.

3. Results and discussion

After the TiN powder was crushed using a three-dimensional crushing machine for 4 h, 8 h, or 12 h, its original size (2 μm) was reduced to 0.303, 0.293, and 0.264 μm, respectively, as listed in Table 2. These results suggested that a longer crushing duration resulted in smaller particles.

However, a partial increase in the particle size occurred after crushing for 8 h and 12 h. This was because the particle size decreased to the nanoscale as the crushing time increased, and the powder particles began to attract one another via van der Waals forces.

For all the tested specimens, the measured resistivities were between 3.11×10^{-3} and $3.65 \times 10^{-3}\,\Omega$ cm, with an average value of $3.26 \times 10^{-3}\,\Omega$ cm and a maximum–minimum disparity factor of 1.17, suggesting that all the test specimens can be machined by EDM. The Vickers hardness was between 1466 and 1603 H_v with a maximum–minimum disparity factor of 1.09. The flexural strength ranged between 574 and 790 MPa and a maximum–minimum disparity varied by a factor of 1.38, as shown in Fig. 2(a). Fig. 2(b) shows the fracture toughness that ranged from 4.06 to 9.28 MPa $m^{1/2}$, with a maximum–minimum disparity factor of 2.28 (a total difference of 5.22 MPa $m^{1/2}$). The relative density, as shown in Fig. 2(c), ranged from 87.4% to 97.2%, with a maximum–minimum disparity factor of 1.11 (a total difference of 9.8%).

On the basis of the above results, the fracture toughness was regarded as the most important factor because a great disparity was observed among all the test specimens. Therefore, when discussing the optimum manufacturing process, fracture toughness must be considered before the flexural strength.

As the S/N ratio variance analysis for fracture toughness (Table 3) showed, Factor A contributed 21.1%; Factor B, 14.3%; Factor C, 55.6%; and Factor D, 9.0%. Because Factor C had the greatest impact on fracture toughness, the optimum-process-parameter setting for Factor C was determined from the S/N ratio response of fracture toughness (Fig. 3(a)). Level 3 was considered the optimum parameter setting for Factor C.

Factor A was believed to be the second most crucial contributing factor to fracture toughness. Fig. 3(b) shows the S/N ratio of flexural strength. Factor A contributed approximately 87.3% to flexural strength, and A3 was also at its optimum value (Fig. 3(b)); therefore, A3 was

considered to be the optimum-process-parameter setting for Factor A.

Factor B's contribution to fracture toughness was 14.3% (Table 3). The fracture toughness response for B2 (16.31 db) was greater than that for B3 (15.35 db) and for B1 (14.75 db), as shown in Fig. 3(a). Level 2 was also the optimum value for fracture strength and flexural strength (Fig. 3(b)); therefore, the optimum-process-parameter setting for Factor B was B2. Factor D's contribution to fracture toughness was 9.0% (Table 3). D1 was considered to be the optimum-process-parameter setting for Factor D (Fig. 3(a)).

According to the analysis of variance to examine each parameter in the manufacturing process, the optimum quality for zirconia-based ceramic containing TiN was achieved using the parameter settings A3, B2, C3, and D1. The optimum process parameters in this experiment consisted of using TiN powder crushed for 8 h and two-step sintering: the sample was sintered at 1450 °C in the first stage without being held at the temperature; the sample was kept at 1150 °C in the second stage for 20 h.

A second experimental verification was completed using the optimum process parameters A3, B2, C3, and D1, which fabricated a 3Y-TZP/TiN ceramic composite with an average fracture toughness of 8.59 MPa $m^{1/2}$ and an average flexural strength of 680.77 MPa. As shown in Table 4, the verified S/N ratio for fracture toughness was 19.57 db, which was only 0.37 db (1.8%) less than the predicted S/N ratio of 19.94 db; the verified S/N ratio for flexural strength was 57.66 db, or 0.21 db (0.36%) less than the predicted S/N ratio of 57.77 db. In summary, the verified values only differed slightly from the predicted values; therefore, it can be concluded that this experimental model is reasonable.

With regard to conventional sintering, the ceramic composite fabricated in Exp. 1 exhibited a higher flexural strength of 602.437 MPa and a lower fracture toughness of 4.055 MPa $m^{1/2}$ than the composite fabricated in Exp. 3 (flexural strength = 574.06 MPa, fracture toughness = 6.34 MPa $m^{1/2}$). In addition, sample ZTN-1 possessed a relatively higher density (90.12%) than sample ZTN-3 (87.36%), as shown in Fig. 2(c). The higher density of ZTN-1 was attributed to the ceramic composite being sintered at 1450 °C for 2 h; hence, ZTN-1 exhibited a higher flexural strength. On the other hand, ZTN-3 contained more material in the tetragonal phase (t-ZrO_2), and therefore, ZTN-3 exhibited higher fracture toughness.

In order to realize the effect of the sintering duration for two-step sintering, the characteristics of the ceramic composite fabricated in Exp. 5 and Exp. 9 were compared. The flexural strength and fracture toughness for ZTN-5

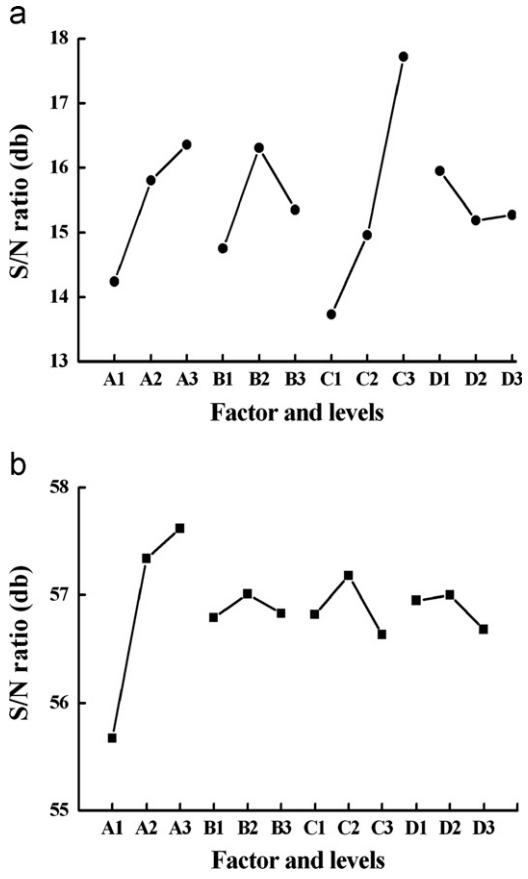

Fig. 3. Factor response to S/N ratio of (a) fracture toughness and (b) flexural strength.

Table 3
Parameter analysis of S/N ratio for fracture toughness and flexural strength.

Fracture toughness					Flexural strength				
Factor	SS	DOF	Var	Contribution	Factor	SS	DOF	Var	Contribution
A	21.86	2	10.93	0.21	A	13.50	2	6.75	0.87
B	14.80	2	7.40	0.14	B	0.32	2	0.16	0.02
C	57.70	2	28.85	0.56	C	1.12	2	0.56	0.07
D	9.39	2	4.69	0.09	D	0.53	2	0.26	0.03
Total	103.74	8	12.97	1	Total	15.47	8	1.93	1

Note: SS (Sum of Square) is the sum of the square of the difference between the measured value and the average value; DOF is the Degree of Freedom; Var is variance.

Table 4
Comparison between verified and predicted S/N ratio for the optimum process parameters of A3, B2, C3, D1.

	The optimum process parameters A3, B2, C3, D1		
	Verified measured average value	Verified S/N ratio	Predicted S/N ratio
Fracture toughness	8.59 MPa $m^{1/2}$	19.57 db	19.94 db
Flexural strength	680.77 MPa	57.56 db	57.77 db

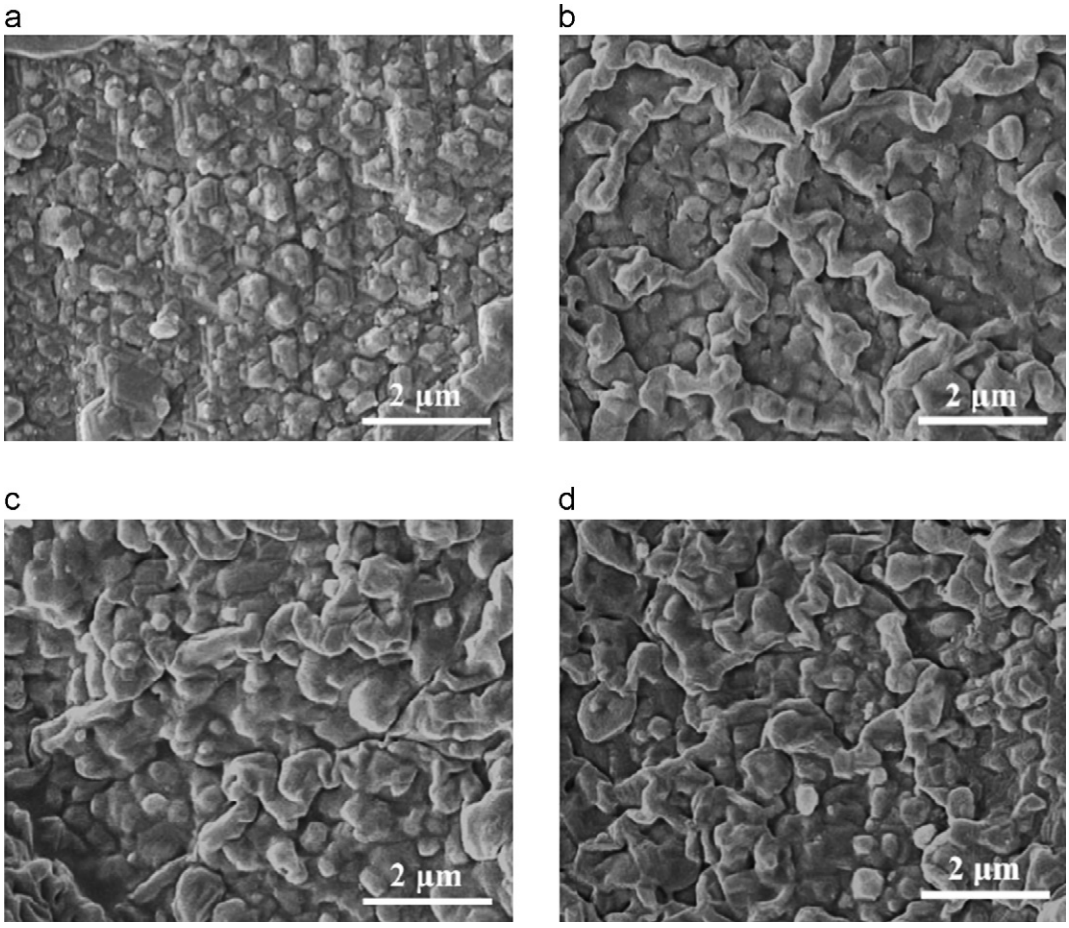

Fig. 4. SEM micrographs of 3Y-TZP/TiN after thermal etching at 1380 °C for 20 min: (a) ZTN-2; (b) ZTN-4; (c) ZTN-6; and (d) ZTN-8.

were 732.30 MPa and 9.28 MPa $m^{1/2}$; the corresponding values for ZTN-9 were 790.13 MPa and 6.42 MPa $m^{1/2}$, respectively. While both used two-step sintering, the temperature of ZTN-5 was not maintained during the first stage, which dropped directly from 1450 °C to 1250 °C in the second stage where it was maintained for 10 h; in Exp. 9, the sample was kept at 1450 °C in the first stage for 1 h and 1250 °C for 20 h in the second stage. Results of the relative densities of ZTN-5 (94.37%) and ZTN-9 (97.22%) indicated that a long duration of sintering efficiently eliminated pores, and hence, ZTN-9 possessed a greater flexural strength. However, ZTN-5 exhibited a greater fracture strength than ZTN-9, primarily because ZTN-5 could retain more t-ZrO_2 since it shifted directly from the first stage to the second stage of sintering, without being kept at a high temperature.

Fig. 4(a)–(d) shows the surface morphologies of the sintered 3Y-TZP/TiN ceramic composite. The SEM micrographs clearly show that zirconia containing TiN could form an electrically conductive mesh-like structure. Furthermore, greater amounts of the mesh-like structures were observed from the ceramic composites fabricated by two-step sintering (Fig. 4(b), (c), and (d)) in comparison with those fabricated by conventional one-step sintering (Fig. 4(a))

Fig. 5 shows the characteristic peaks of 3Y-TZP (t-ZrO_2 and m-ZrO_2) and TiN, which were identified from the X-ray diffraction patterns. The relative amounts of t-ZrO_2

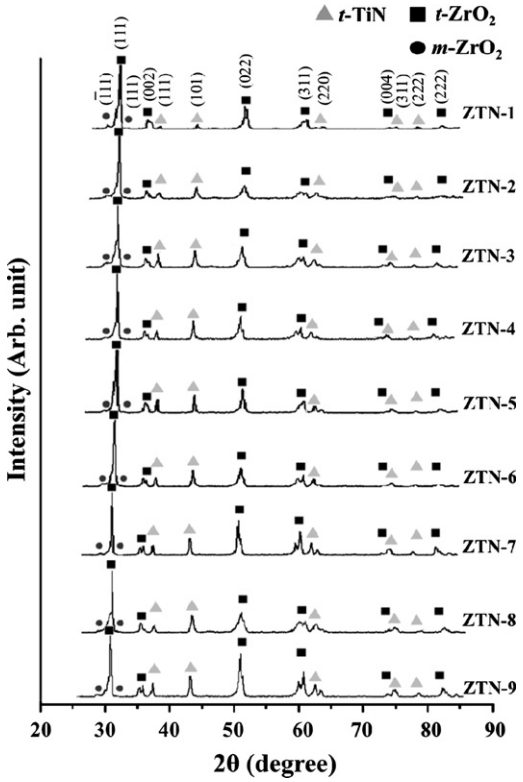

Fig. 5. X-ray diffraction patterns for different process parameters.

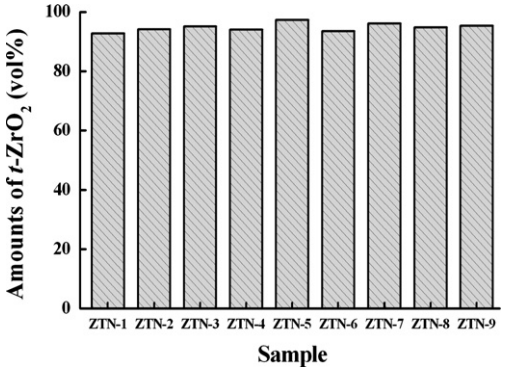

Fig. 6. The relative amounts of t-ZrO_2 containing in the sintered ceramic composites.

and m-ZrO_2 were calculated and are illustrated in Fig. 6, which indicated that the volume percent of t-ZrO_2, mainly depended on the sintering duration. For example, when the temperature was not maintained during the first sintering stage, but dropped directly to the second stage sintering temperature (ZTN-3, -5, and -7), the sintered ceramic composites contained more t-ZrO_2. As shown in Fig. 6, the volume percent of ZTN-3, ZTN-5, and ZTN-7 was 95.2%, 97.3% and 96.1%, respectively. Therefore, the sintered ceramic composites fabricated in Exp. 3, 5, and 7 possessed greater fracture toughness. In contrast, the higher the temperature and the longer it was maintained, the greater was the flexural strength because the sintering density increased with the sintering duration.

4. Conclusions

This study successfully fabricated an electrically conductive zirconia by adding 30 wt% TiN. The mesh-like structures were suggested as the conductive paths. The fracture toughness and flexural strength of the sintered ceramic composites were found to depend on the t-ZrO_2 amounts and bulk density, respectively. Furthermore, using the Taguchi method, the optimum manufacturing parameters were obtained, i.e., two-step sintering with a first stage that did not maintain temperature, a second stage that maintained a temperature of 1250 °C for 20 h, and a TiN crushing time of 8 h. Using these parameters, the sintered ceramic composite achieved an average fracture toughness of 8.59 MPa $m^{1/2}$ and an average flexural strength of 680.77 MPa. The electric resistance for the 3Y-TZP/TiN was $3.26 \times 10^{-3}\,\Omega\,cm$, which could be electric-discharge machining.

References

[1] J.L. Shi, B.S. Li, Z.L. Lu, X.X. Huang, Correlation between microstructure, phase transformation during fracture and the mechanical properties of Y-TZP ceramics, Journal of the European Ceramic Society 16 (1996) 795–798.
[2] S.R. Jansen, A.J.A. Winnubst, Y.J. He, P.G.Th. Varst van de, G. With de, Effects of grain size and ceria addition on ageing behaviour and tribological properties of Y-TZP ceramics, Journal of the European Ceramic Society 18 (1998) 557–563.
[3] W.J. Tseng, M. Taniguchi, T. Yamada, Transformation strengthening of as-fired zirconia ceramics, Ceramics International 25 (1999) 545–550.
[4] K. Vanmeensel, A. Laptev, O. Van der Biest, J. Vleugels, The influence of percolation during pulsed electric current sintering of ZrO_2–TiN powder compacts with varying TiN content, Acta Materialia 55 (2007) 1801–1811.
[5] K. Bonny, P. De Baets, J. Vleugel, A. Salehi, O. Van der Biest, B. Lauwers, W. Liu, Influence of secondary electro-conductive phases on the electrical discharge machinability and frictional behavior of ZrO_2-based ceramic composites, Journal of Materials Processing Technology 208 (2008) 423–430.
[6] I. Puertas, C.J. Luis, A revision of the applications of the electrical discharge machining process to the manufacture of conductive ceramics, Revista de Metalurgia 38 (5) (2002) 358–372.
[7] B. Lauwers, K. Brans, W. Liu, J. Vleugels, S. Salehi, K. Vanmeensel, Influence of the type and grain size of the electro-conductive phase on the wire-EDM performance of ZrO_2 ceramic composites, CIRP Annals—Manufacturing Technology 57 (2008) 191–194.
[8] I. Puertas, C.J. Luis, A study on the electrical discharge machining of conductive ceramics, Journal of Materials Processing Technology 153–154 (2004) 1033–1038.
[9] Y. Perez Delgado, K. Bonny, P. De Baets, P.D. Neis, O. Malek, J. Vleugels, B. Lauwers, Impact of wire-EDM on dry sliding friction and wear of WC-based and ZrO_2-based composites, Wear 271 (2011) 1951–1961.
[10] B. Lauwers, J.P. Kruth, W. Liu, W. Eeraerts, B. Schacht, P. Bleys, Investigation of material removal mechanisms in EDM of composite ceramic materials, Journal of Materials Processing Technology 149 (2004) 347–352.

[11] A. Bravo-Leon, Y. Morikawa, M. Kawahara, M.J. Mayo, Fracture toughness of nanocrystalline tetragonal zirconia with low yttria content, Acta Materialia 50 (2002) 4555–4562.

[12] K. Shibata, R. Sato, M. Yoshinaka, K. Hirota, O. Yamaguchi, Electrical and mechanical properties of ZrO_2(2Y)/TiN composites and laminates made from these materials, Journal of Materials Science 32 (1997) 583–587.

[13] S. Ran, L. Gao, Mechanical properties and microstructure of TiN/TZP nanocomposites, Materials Science and Engineering: A 447 (2007) 83–86.

[14] V. Jef, O. Van der Biest, Development and characterization of Y_2O_3-stabilized ZrO_2 (Y-TZP) composites with TiB_2, TiN, TiC, and $TiC_{0.5}N_{0.5}$, Journal of the American Ceramic Society 82 (10) (1999) 2717–2720.

[15] K. Bonny, P. De Baets, W. Ost, Y. Perez, J. Vleugels, O. Van der Biest, W. Liu, B. Lauwers, Influence of secondary phases on the tribological response of electro-discharge machined zirconia-based composites against WC–Co cemented carbide, Wear 267 (2009) 2157–2166.

[16] S. Lopez-Esteban, C.F. Gutierrez-Gonzalez, G. Mata-Osoro, C. Pecharroman, L.A. Diaz, R. Torrecillas, Electrical discharge machining of ceramic/semiconductor/metal nanocomposites, Scripta Materialia 63 (2010) 219–222.

[17] K. Niihara, R. Morena, D.P.H. Hasselman, Evaluation of K_{IC} of brittle solids by the indentations method with low crack-to-indent ratios, Journal of Materials Science Letters 1 (1982) 13–16.